# The Simultaneous Interpolation of Antenna Radiation Patterns in Both the Spatial and Frequency Domains Using Model-Based Parameter Estimation

Douglas H. Werner, *Senior Member, IEEE,* and Rene J. Allard

***Abstract*—The Padé rational function fitting model commonly used for model-based parameter estimation (MBPE) in the frequency domain is enhanced to include spatial dependence in the numerator and denominator coefficients. This allows the function to interpolate an antenna radiated electric field pattern in both the frequency and spatial domains simultaneously, such that a single set of coefficients can be used to accurately reconstruct an entire radiation pattern at any frequency in the fitting-model range. A simple procedure is introduced for transforming interpolated electric fields into gain patterns using input impedance versus frequency curves also obtained via MBPE. The utility of this method is demonstrated by applying it to a dipole antenna over a frequency range of 150–950 MHz and using a polynomial representation in $\theta$ for the coefficient spatial dependence. It is also used to estimate radiation patterns for a three-element Yagi array between the frequencies of 470 and 500 MHz using a binomial representation for the spatial variation that includes terms dependent on $\theta$ as well as $\phi$. The use of this method for interpolating radiation patterns has at least two significant advantages; one being large compression ratios for the amount of data that must be stored to accurately reproduce patterns and the other being a significant decrease in the amount of time required for modeling problems with large computational domains.**

***Index Terms*—Antenna radiation patterns, model-based parameter estimation.**

## I. Introduction

THE process of creating a large database of antenna radiation patterns containing both spatial and frequency domain information can be an arduous task, especially when considering the amount of space on storage media required to accurately reproduce these patterns. A typical high-fidelity radiation pattern will contain more than 64 000 data points in its spatial domain representation alone. If information on how this pattern changes as a function of frequency is desired, the only solution currently available is to store an entire spatial pattern for every frequency within the operational range of the antenna. Clearly, a scheme whereby high-fidelity radiation patterns can be interpolated, compressed, and then regenerated at differing levels of fidelity in both space and frequency is highly desirable. In many cases, including those concerned with only the spatial variation of antenna radiation patterns, interpolation can be done using the multitude of curve and surface fitting algorithms available [1], which often incorporate polynomial and binomial fitting models for one- and two-dimensional curves and surfaces, respectively. For some situations, however, such as frequency dependence in the case of radiation patterns, these functions are not sufficient to represent the data in question and an interpolation model must be chosen, which takes into account the physics behind the problem. Such models fall into a class of data-fitting algorithms known as model-based parameter estimation (MBPE).

A series of articles by Miller [2]–[5] describes in detail the theory behind the MBPE interpolation process and gives many examples to which it may be applied. In [2] and [3], the motivation for using physically based model equations to represent parameters in electromagnetics applications is given, along with a detailed tabulation of many different types of model-based equations, which are in common use. The modeling, sampling, and solution of MBPE problems for both spatial and frequency domain problems, including the use of matrix inversion techniques to solve for the interpolation coefficients, is described in [4]. Specific applications to antennas are considered, including the use of MBPE to interpolate the input impedance of an antenna as a function of the operating frequency. Other applications mentioned for MBPE are the filtering of noisy data, the determination of scattering patterns from antennas, antenna radiation pattern analysis and synthesis, and schemes for choosing optimum data sampling. A procedure for combining MBPE with the method of moments (MoM) that leads to an efficient technique for solving electric field integral equations (EFIE's) is outlined in [5]. In [6], the use of MBPE is discussed for reducing numerical error or error due to inadequacies in parameter estimation and, in [7], the concept of optimized sampling is presented in some detail with particular emphasis placed on frequency domain applications. A method for using MBPE to model the spatial dependence of antenna radiation patterns is given by Miller in [8], with the objective of reducing the number of sampling points needed to accurately represent radiation and scattering patterns for antennas. Finally, Roberts and McNamara have demonstrated in [9] that MBPE can also be successfully used to synthesize antenna radiation patterns at a single frequency by determining the array currents necessary to produce a desired pattern.

In discussing frequency domain applications of MBPE, [2]–[5] make use of the Padé rational function. As pointed out by Press *et al.* [10], functions such as this one are more useful than simple polynomials or binomial models in some cases because they are able to represent complicated pole-zero

Manuscript received August 5, 1998; revised December 3, 1999. This work was supported by the Naval Information Warfare Activity (NIWA), Washington, DC.

The authors are with the Applied Research Laboratory, Pennsylvania State University, State College, PA 16804 USA.

Publisher Item Identifier S 0018-926X(00)02449-2.

functional forms. This procedure is know as Padé approximation. Spectral response curves are known to exhibit this type of behavior, which suggests that the Padé rational function is a logical choice to use for the interpolation of frequency dependent data sets. For example this type of function is used in [4] to interpolate the input impedance of an antenna as a function of frequency. The model-order reduction that is possible when using a rational function, as opposed to what would be possible if a polynomial or other nonphysical function were used, is also demonstrated in [4]. While MBPE techniques have been successfully applied to the interpolation of antenna input impedance as demonstrated in [4], there has not been any documented attempt to extend these techniques to include interpolation of the corresponding frequency variation in the radiation patterns.

The purpose of this paper is to present a generalized Padé rational function fitting model that can be used to interpolate both frequency and spatial characteristics of antenna radiation patterns simultaneously. Although simple polynomial and binomial functions cannot model accurately the pole-zero structure of the frequency response, they are quite capable of interpolating the spatial structure of the radiation pattern at a single frequency. A hybrid method for combining a rational function pole-zero frequency domain fitting model with a polynomial or binomial spatial domain fitting model is introduced in this paper. This new hybrid method allows an antenna radiation pattern to be interpolated in both the spatial and frequency domains simultaneously such that only a single set of coefficients is necessary to reconstruct the entire pattern of interest with any desired angular resolution and at any frequency within the operational range of the antenna. Two practical examples are considered in this paper which serve to demonstrate the utility of this new hybrid MBPE technique. In particular, the hybrid MBPE approach will be shown to yield accurate reproductions of radiation patterns for a 0.5-m dipole, modeled from 150–950 MHz, and a three-element Yagi antenna, modeled from 470–500 MHz, at several different frequencies within the range of each interpolation model.

## II. Theory

MBPE is a form of "smart" curve fitting because it uses a fitting model, which is based on the problem physics as opposed to standard curve-fitting techniques that do not make use of the problem physics and, consequently, tend to be much less efficient. The "model-based" part of MBPE involves using low-order analytical formulas as fitting models, while the "parameter estimation" part refers to the process of numerically obtaining coefficients for the fitting model by matching it or fitting it to sampled values (either calculated or measured). One form of a fitting model that is commonly employed in MBPE is represented by the rational function [4], [5]

$$F(s)=\frac{N(s)}{D(s)}=\frac{N_0+N_1s+N_2s^2+\cdots+N_ns^n}{D_0+D_1s+D_2s^2+\cdots+D_{d-1}s^{d-1}+s^d} \quad (1)$$

where $F(s)$ represents a spectral-domain fitting model (SD FM) appropriate for the set of complex data undergoing interpolation, the argument $s$ represents the complex frequency $j\omega$ and the function has $n+d+1$ unknown complex coefficients [2], [4], [5]. By sampling $F(s)$ at a total of $Nf$ frequencies, the expression in (1) can be written as a matrix equation of the form

$$\boldsymbol{A}\boldsymbol{x}=\boldsymbol{b} \quad (2)$$

where $\boldsymbol{A}$ and $\boldsymbol{b}$ are shown in (3), shown at the bottom of the page, and

$$\boldsymbol{b}=\begin{bmatrix} F(s_1)s_1^d \\ F(s_2)s_2^d \\ \vdots \\ F(s_{Nf})s_{Nf}^d \end{bmatrix}. \quad (4)$$

and the coefficient matrix is given by

$$\boldsymbol{x}=\begin{bmatrix} N_0 \\ N_1 \\ \vdots \\ N_n \\ D_0 \\ D_1 \\ \vdots \\ D_{d-1} \end{bmatrix}. \quad (5)$$

This matrix equation may then be solved in order to determine the set of appropriate numerator and denominator coefficients for (1).

The Padé rational function (1) has been successfully used in the past to interpolate antenna input impedance $Z_{\mathbf{in}}$ versus frequency by setting $F(s)$ equal to the sampled values of the impedance and $s=j\omega=j2\pi f$, where $f$ is the frequency at which the antenna is operated [2], [4], [5]. This paper, however, is concerned with developing a MBPE scheme for the efficient interpolation of antenna radiation patterns. In order to accomplish this, the methods proposed in [2], [4], [5] must be extended to include not only frequency variation but also spatial variation. This would allow radiation patterns to be reconstructed via the MBPE interpolation at any frequency within the predetermined operational range of the antenna. One approach for ac-

$$\boldsymbol{A}=\begin{bmatrix} 1 & s_1 & \cdots & s_1^n & -F(s_1) & -F(s_1)s_1 & \cdots & -F(s_1)s_1^{d-1} \\ 1 & s_2 & \cdots & s_2^n & -F(s_2) & -F(s_2)s_2 & \cdots & -F(s_2)s_2^{d-1} \\ \vdots & \vdots & \vdots & \vdots & \vdots & \vdots & \vdots & \vdots \\ 1 & s_{Nf} & \cdots & s_{Nf}^n & -F(s_{Nf}) & -F(s_{Nf})s_{Nf} & \cdots & -F(s_{Nf})s_{Nf}^{d-1} \end{bmatrix} \quad (3)$$

complishing this would be to use the rational function (1) to interpolate the frequency response of the complex far-zone radiated electric field at a particular value of $\theta$ and $\phi$ [11], [12]. This technique may be applied repeatedly over a range of values for $\theta$ and $\phi$ in order to obtain an approximation for the radiation pattern at any desired frequency. However, one major drawback of this technique is that it is not very computationally efficient because it requires very fine sampling resolution in the spatial domain. This is true because in order to provide a complete set of high-fidelity spatial radiation patterns at each frequency within the model range, a separate MBPE interpolation must be performed at every point in space where radiation pattern data is desired. To obtain accurate spatial resolution, the number of separate interpolations required and, therefore, the overall number of resulting interpolation coefficients becomes very large. A much better approach is to assume that the numerator and denominator coefficients of (1) are functions of the spatial domain angles. This assumption allows interpolation to be performed in the spatial domain as well as in the frequency domain. Therefore, a much smaller number of spatial sampling points can be used to provide the same level of resolution obtained via the technique described in [11] and [12] while requiring far fewer interpolation coefficients. For instance, we may write (1) in the more general form

$$\begin{aligned} F(\theta, s) &= \frac{N(\theta, s)}{D(\theta, s)} \\ &= \frac{N_0(\theta)+N_1(\theta)s+N_2(\theta)s^2+\cdots+N_n(\theta)s^n}{D_0(\theta)+D_1(\theta)s+D_2(\theta)s^2+\cdots+D_{d-1}(\theta)s^{d-1}+s^d} \end{aligned} \tag{6}$$

where the $n+d+1$ unknown numerator and denominator coefficients now possess dependence on a spatial variable, in this case $\theta$ and thus (6) can be used to interpolate antenna radiation patterns as a function of both frequency and angle simultaneously. There are several possible models, which could be adopted to represent the dependence of these coefficients on angle. For the purpose of this study we have chosen to consider a simple polynomial model of the form

$$\begin{aligned} N_0(\theta) &= N_0^0 + N_0^1\theta + N_0^2\theta^2 + \cdots + N_0^k\theta^k \\ N_1(\theta) &= N_1^0 + N_1^1\theta + N_1^2\theta^2 + \cdots + N_1^k\theta^k \\ &\vdots \\ N_n(\theta) &= N_n^0 + N_n^1\theta + N_n^2\theta^2 + \cdots + N_n^k\theta^k \\ \\ D_0(\theta) &= D_0^0 + D_0^1\theta + D_0^2\theta^2 + \cdots + D_0^k\theta^k \\ D_1(\theta) &= D_1^0 + D_1^1\theta + D_1^2\theta^2 + \cdots + D_1^k\theta^k \\ &\vdots \\ D_{d-1}(\theta) &= D_{d-1}^0 + D_{d-1}^1\theta + D_{d-1}^2\theta^2 + \cdots + D_{d-1}^k\theta^k \end{aligned} \tag{7}$$

where $k$ represents the polynomial order for each Padé coefficient.

By sampling the set of calculated or measured complex electric field data at $Nf$ frequency points and, at $N\theta$ points in space, a matrix equation of the form given in (2) can be constructed where $\boldsymbol{A}$ and $\boldsymbol{b}$ are given by (8), shown at the bottom of the next page, and

$$\boldsymbol{b} = \begin{bmatrix} F(\theta_1, s_1)s_1^d \\ F(\theta_1, s_2)s_2^d \\ \vdots \\ F(\theta_1, s_{Nf})s_{Nf}^d \\ F(\theta_2, s_1)s_1^d \\ F(\theta_2, s_2)s_2^d \\ \vdots \\ F(\theta_2, s_{Nf})s_{Nf}^d \\ \vdots \\ F(\theta_{N\theta}, s_1)s_1^d \\ F(\theta_{N\theta}, s_2)s_2^d \\ \vdots \\ F(\theta_{N\theta}, s_{Nf})s_{Nf}^d \end{bmatrix}. \tag{9}$$

respectively, and $F(\theta_i, s_j)$ represents the value of the complex electric field at a particular sampling point. The corresponding coefficient matrix $\boldsymbol{x}$ is composed of the $Nf \times N\theta$ unknown complex coefficients given by

$$\boldsymbol{x} = \begin{bmatrix} \overline{\boldsymbol{N}}_{\boldsymbol{0}} \\ \overline{\boldsymbol{N}}_{\boldsymbol{1}} \\ \vdots \\ \overline{\boldsymbol{N}}_{\boldsymbol{n}} \\ \overline{\boldsymbol{D}}_{\boldsymbol{0}} \\ \overline{\boldsymbol{D}}_{\boldsymbol{1}} \\ \vdots \\ \overline{\boldsymbol{D}}_{\boldsymbol{d-1}} \end{bmatrix} \tag{10}$$

where $\overline{\boldsymbol{N}}_{\boldsymbol{i}} = [N_i^0 N_i^1 N_i^2 \cdots N_i^k]^{\boldsymbol{T}}$ for $i = 0, 1, \cdots, n$ and $\overline{\boldsymbol{D}}_{\boldsymbol{j}} = [D_j^0 D_j^1 D_j^2 \cdots D_j^k]^{\boldsymbol{T}}$ for $j = 0, 1, \cdots, d-1$. Solving this matrix equation yields the set of numerator and denominator coefficients required by (6).

The fitting model proposed in (6) may be easily extended to include radiation patterns which not only have a dependence on $\theta$, but also vary with $\phi$. The general form of the fitting model under these conditions will be as shown in (11), on p. 387. In this case, we choose to approximate the numerator and denominator coefficients by the following binomial expansions [1]:

$$N_i(\theta, \phi) = \sum_{j=1}^{P_n+1} \sum_{k=1}^{j} N_i^{(j-k, k-1)} \theta^{j-k} \phi^{k-1} \tag{12}$$

$$D_l(\theta, \phi) = \sum_{m=1}^{P_n+1} \sum_{n=1}^{m} D_l^{(m-n, n-1)} \theta^{m-n} \phi^{n-1} \tag{13}$$

where $P_n$ is the class of the binomial, or the highest power of $\theta$ and $\phi$ present in the binomial expansion. For a given binomial class, the number of coefficients present in the expansion is

$$C = \frac{(P_n+1)(P_n+2)}{2} \tag{14}$$

and when fully expanded the coefficient functions (12) and (13) become

$$
\begin{aligned}
N_0(\theta,\phi) &= N_0^{(0,0)} + N_0^{(1,0)}\theta + N_0^{(0,1)}\phi + N_0^{(2,0)}\theta^2 \\
&\quad + N_0^{(1,1)}\theta\phi + N_0^{(0,2)}\phi^2 + \cdots + N_0^{(P_n,0)}\theta^{P_n} \\
&\quad + \cdots + N_0^{(0,P_n)}\phi^{P_n} \\
N_1(\theta,\phi) &= N_1^{(0,0)} + N_1^{(1,0)}\theta + N_1^{(0,1)}\phi + N_1^{(2,0)}\theta^2 \\
&\quad + N_1^{(1,1)}\theta\phi + N_1^{(0,2)}\phi^2 + \cdots + N_1^{(P_n,0)}\theta^{P_n} \\
&\quad + \cdots + N_1^{(0,P_n)}\phi^{P_n} \\
&\vdots \\
N_n(\theta,\phi) &= N_n^{(0,0)} + N_n^{(1,0)}\theta + N_n^{(0,1)}\phi + N_n^{(2,0)}\theta^2 \\
&\quad + N_n^{(1,1)}\theta\phi + N_n^{(0,2)}\phi^2 + \cdots + N_n^{(P_n,0)}\theta^{P_n} \\
&\quad + \cdots + N_n^{(0,P_n)}\phi^{P_n} \\
D_0(\theta,\phi) &= D_0^{(0,0)} + D_0^{(1,0)}\theta + D_0^{(0,1)}\phi + D_0^{(2,0)}\theta^2 \\
&\quad + D_0^{(1,1)}\theta\phi + D_0^{(0,2)}\phi^2 + \cdots + D_0^{(P_n,0)}\theta^{P_n} \\
&\quad + \cdots + D_0^{(0,P_n)}\phi^{P_n} \\
D_1(\theta,\phi) &= D_1^{(0,0)} + D_1^{(1,0)}\theta + D_1^{(0,1)}\phi + D_1^{(2,0)}\theta^2 \\
&\quad + D_1^{(1,1)}\theta\phi + D_1^{(0,2)}\phi^2 + \cdots + D_1^{(P_n,0)}\theta^{P_n} \\
&\quad + \cdots + D_1^{(0,P_n)}\phi^{P_n} \\
&\vdots \\
D_{d-1}(\theta,\phi) &= D_{d-1}^{(0,0)} + D_{d-1}^{(1,0)}\theta + D_{d-1}^{(0,1)}\phi + D_{d-1}^{(2,0)}\theta^2 \\
&\quad + D_{d-1}^{(1,1)}\theta\phi + D_{d-1}^{(0,2)}\phi^2 + \cdots + D_{d-1}^{(P_n,0)}\theta^{P_n} \\
&\quad + \cdots + D_{d-1}^{(0,P_n)}\phi^{P_n}. \qquad (15)
\end{aligned}
$$

As in the previous case, the rational function defined by (11) is expanded using the set of coefficients given in (15) and then sampled at the appropriate number of data points in order to construct a matrix equation of the form (2). The total number of sampling points for this matrix is $N\theta \times N\phi \times Nf$ where $N\theta$ and $N\phi$ represent the total number of sampling points in $\theta$ and $\phi$,

$$
\boldsymbol{A} = \begin{bmatrix}
1 & \theta_1 & \cdots & \theta_1^k & s_1 & \theta_1 s_1 & \cdots & \theta_1^k s_1 & \cdots & s_1^n & \theta_1 s_1^n & \cdots & \theta_1^k s_1^n & -F(\theta_1, s_1) & \cdots \\
1 & \theta_1 & \cdots & \theta_1^k & s_2 & \theta_1 s_2 & \cdots & \theta_1^k s_2 & \cdots & s_2^n & \theta_1 s_2^n & \cdots & \theta_1^k s_2^n & -F(\theta_1, s_2) & \cdots \\
\vdots & & & & & & \vdots & & & & & \vdots & & & \\
1 & \theta_1 & \cdots & \theta_1^k & s_{Nf} & \theta_1 s_{Nf} & \cdots & \theta_1^k s_{Nf} & \cdots & s_{Nf}^n & \theta_1 s_{Nf}^n & \cdots & \theta_1^k s_{Nf}^n & -F(\theta_1, s_{Nf}) & \cdots \\
1 & \theta_2 & \cdots & \theta_2^k & s_1 & \theta_2 s_1 & \cdots & \theta_2^k s_1 & \cdots & s_1^n & \theta_2 s_1^n & \cdots & \theta_2^k s_1^n & -F(\theta_2, s_1) & \cdots \\
1 & \theta_2 & \cdots & \theta_2^k & s_2 & \theta_2 s_2 & \cdots & \theta_2^k s_2 & \cdots & s_2^n & \theta_2 s_2^n & \cdots & \theta_2^k s_2^n & -F(\theta_2, s_2) & \cdots \\
\vdots & & & & & & \vdots & & & & & \vdots & & & \\
1 & \theta_2 & \cdots & \theta_2^k & s_{Nf} & \theta_2 s_{Nf} & \cdots & \theta_2^k s_{Nf} & \cdots & s_{Nf}^n & \theta_2 s_{Nf}^n & \cdots & \theta_2^k s_{Nf}^n & -F(\theta_2, s_{Nf}) & \cdots \\
\vdots & & & & & & \vdots & & & & & \vdots & & & \\
1 & \theta_{N\theta} & \cdots & \theta_{N\theta}^k & s_1 & \theta_{N\theta} s_1 & \cdots & \theta_{N\theta}^k s_1 & \cdots & s_1^n & \theta_{N\theta} s_1^n & \cdots & \theta_{N\theta}^k s_1^n & -F(\theta_{N\theta}, s_1) & \cdots \\
1 & \theta_{N\theta} & \cdots & \theta_{N\theta}^k & s_2 & \theta_{N\theta} s_2 & \cdots & \theta_{N\theta}^k s_2 & \cdots & s_2^n & \theta_{N\theta} s_2^n & \cdots & \theta_{N\theta}^k s_2^n & -F(\theta_{N\theta}, s_2) & \cdots \\
\vdots & & & & & & \vdots & & & & & \vdots & & & \\
1 & \theta_{N\theta} & \cdots & \theta_{N\theta}^k & s_{Nf} & \theta_{N\theta} s_{Nf} & \cdots & \theta_{N\theta}^k s_{Nf} & \cdots & s_{Nf}^n & \theta_{N\theta} s_{Nf}^n & \cdots & \theta_{N\theta}^k s_{Nf}^n & -F(\theta_{N\theta}, s_{Nf}) & \cdots
\end{bmatrix}
$$

$$
\begin{bmatrix}
-F(\theta_1, s_1)\theta_1^k & -F(\theta_1, s_1)s_1 & \cdots & -F(\theta_1, s_1)\theta_1^k s_1 & \cdots & -F(\theta_1, s_1)s_1^{d-1} & \cdots & -F(\theta_1, s_1)\theta_1^k s_1^{d-1} \\
-F(\theta_1, s_2)\theta_1^k & -F(\theta_1, s_2)s_2 & \cdots & -F(\theta_1, s_2)\theta_1^k s_2 & \cdots & -F(\theta_1, s_2)s_2^{d-1} & \cdots & -F(\theta_1, s_2)\theta_1^k s_2^{d-1} \\
\vdots & & & & \vdots & & & \vdots \\
-F(\theta_1, s_{Nf})\theta_1^k & -F(\theta_1, s_{Nf})s_{Nf} & \cdots & -F(\theta_1, s_{Nf})\theta_1^k s_{Nf} & \cdots & -F(\theta_1, s_{Nf})s_{Nf}^{d-1} & \cdots & -F(\theta_1, s_{Nf})\theta_1^k s_{Nf}^{d-1} \\
-F(\theta_2, s_1)\theta_2^k & -F(\theta_2, s_1)s_1 & \cdots & -F(\theta_2, s_1)\theta_2^k s_1 & \cdots & -F(\theta_2, s_1)s_1^{d-1} & \cdots & -F(\theta_2, s_1)\theta_2^k s_1^{d-1} \\
-F(\theta_2, s_2)\theta_2^k & -F(\theta_2, s_2)s_2 & \cdots & -F(\theta_2, s_2)\theta_2^k s_2 & \cdots & -F(\theta_2, s_2)s_2^{d-1} & \cdots & -F(\theta_2, s_2)\theta_2^k s_2^{d-1} \\
\vdots & & & & \vdots & & & \vdots \\
-F(\theta_2, s_{Nf})\theta_2^k & -F(\theta_2, s_{Nf})s_{Nf} & \cdots & -F(\theta_2, s_{Nf})\theta_2^k s_{Nf} & \cdots & -F(\theta_2, s_{Nf})s_{Nf}^{d-1} & \cdots & -F(\theta_2, s_{Nf})\theta_2^k s_{Nf}^{d-1} \\
\vdots & & & & \vdots & & & \vdots \\
-F(\theta_{N\theta}, s_1)\theta_{N\theta} & -F(\theta_{N\theta}, s_1)s_1 & \cdots & -F(\theta_{N\theta}, s_1)\theta_{N\theta}^k s_1 & \cdots & -F(\theta_{N\theta}, s_1)s_1^{d-1} & \cdots & -F(\theta_{N\theta}, s_1)\theta_{N\theta}^k s_1^{d-1} \\
-F(\theta_{N\theta}, s_2)\theta_{N\theta} & -F(\theta_{N\theta}, s_2)s_2 & \cdots & -F(\theta_{N\theta}, s_2)\theta_{N\theta}^k s_2 & \cdots & -F(\theta_{N\theta}, s_2)s_2^{d-1} & \cdots & -F(\theta_{N\theta}, s_2)\theta_{N\theta}^k s_2^{d-1} \\
\vdots & & & & \vdots & & & \vdots \\
-F(\theta_{N\theta}, s_{Nf})\theta_{N\theta} & -F(\theta_{N\theta}, s_{Nf})s_{Nf} & \cdots & -F(\theta_{N\theta}, s_{Nf})\theta_{N\theta}^k s_{Nf} & \cdots & -F(\theta_{N\theta}, s_{Nf})s_{Nf}^{d-1} & \cdots & -F(\theta_{N\theta}, s_{Nf})\theta_{N\theta}^k s_{Nf}^{d-1}
\end{bmatrix}
\qquad (8)
$$

respectively, and $Nf$ is the total number of frequency sampling points. The coefficient matrix $\boldsymbol{x}$ in this case is given by

$$\boldsymbol{x} = \begin{bmatrix} \overline{\boldsymbol{N}}_{\boldsymbol{0}} \\ \overline{\boldsymbol{N}}_{\boldsymbol{1}} \\ \vdots \\ \overline{\boldsymbol{N}}_{\boldsymbol{n}} \\ \overline{\boldsymbol{D}}_{\boldsymbol{0}} \\ \overline{\boldsymbol{D}}_{\boldsymbol{1}} \\ \vdots \\ \overline{\boldsymbol{D}}_{\boldsymbol{d-1}} \end{bmatrix} \tag{16}$$

where

$$\overline{\boldsymbol{N}}_{\boldsymbol{i}} = [N_i^{(0,0)}\ N_i^{(1,0)}\ N_i^{(0,1)}\ N_i^{(2,0)}\ N_i^{(1,1)}\ N_i^{(0,2)}\ N_i^{(3,0)}\ \cdots\ N_i^{(0,3)}\ \cdots\ N_i^{(P_n,0)}\ \cdots\ N_i^{(0,P_n)}]^{\boldsymbol{T}}$$

for

$$i = 0,\ 1,\ \cdots,\ n$$

and

$$\overline{\boldsymbol{D}}_{\boldsymbol{j}} = [D_j^{(0,0)}\ D_j^{(1,0)}\ D_j^{(0,1)}\ D_j^{(2,0)}\ D_j^{(1,1)}\ D_j^{(0,2)}\ D_j^{(3,0)}\ \cdots\ D_j^{(0,3)}\ \cdots\ D_j^{(P_n,0)}\ \cdots\ D_j^{(0,P_n)}]^{\boldsymbol{T}}$$

for $j = 0,\ 1,\ \cdots,\ d-1$ and the total number of unknown coefficients is $\frac{1}{2}(P_n+1)(P_n+2)(n+d+1)$.

The methods described above are used to interpolate complex electric field values, but in many cases it is the antenna gain pattern that is of the greatest interest. Therefore, a technique for efficiently converting the interpolated electric field values to gain is outlined below. The technique is based on the fact that the gain of an antenna may be expressed in the form [13]

$$G(\theta,\ \phi) = \frac{4\pi U(\theta,\ \phi)}{P_{\text{in}}} \tag{17}$$

where

$$P_{\text{in}} = \tfrac{1}{2}\,\text{Re}\,\{V_{\text{in}} I_{\text{in}}^*\} = \tfrac{1}{2}\,|I_{\text{in}}|^2\,R_{\text{in}} \tag{18}$$

and

$$U(\theta,\ \phi) = \frac{r^2}{2\eta_0}\left(|E_\theta|^2 + |E_\phi|^2\right) \tag{19}$$

which represent the input power accepted by the antenna and the antenna radiation intensity, respectively. The complex-valued input current to the antenna is given by

$$I_{\text{in}} = \frac{V_a}{Z_{\text{in}}} \tag{20}$$

where $V_a$ is the excitation voltage applied to the antenna and $Z_{\text{in}}$ is the antenna input impedance. A technique for interpolating the input impedance of an antenna via Padé approximations has been demonstrated previously by Miller [2]–[4]. A similar technique may be employed here which uses Padé approximations to estimate the input impedance $Z_{\text{in}} = R_{\text{in}} + jX_{\text{in}}$ required in order to calculate the input power $P_{\text{in}}$ (18) of a particular antenna as a function of frequency. Finally, the interpolated electric field values may be used to calculate (19) and, ultimately, the required antenna gain (17).

## III. Results

The MBPE techniques described in the previous section were first applied to a 0.5-m dipole antenna over a frequency range of 150–950 MHz, using radiation pattern data obtained from a numerically rigorous method of moments (MoM) computer code. Since the dipole is oriented along the $z$-axis, there will be no $\phi$-variation in the radiation pattern. This suggests that a rational function fitting model of the type given in (6), which only depends on a single angular variable $\theta$, would be sufficient for interpolating the radiation pattern. Furthermore, the symmetry of the problem may be exploited such that it is only necessary to apply the interpolation over the limited range $0° \le \theta \le 90°$. The rational function was chosen to have a numerator order $n = 4$, a denominator order $d = 2$, and a polynomial coefficient order $k = 7$. The fitting frequencies selected were 150, 300, 350, 600, 800, 900, and 950 MHz, and the fitting angles for the spatial dependence were chosen to be 2, 10, 20, 40, 50, 60, 80, and 90°. These parameters, including the frequency and spatial domain sampling points and the Padé and polynomial function interpolation orders were chosen experimentally by varying the parameter values and selecting those which produced the best results. This information was used to construct a matrix of the form given in (8) where, in this case, $Nf = n + d + 1 = 7$ and $N\theta = k + 1 = 8$. The required $Nf \times N\theta = 56$ unknown coefficients for (6) were determined by solving the related matrix equation (2) using (8)–(10). A surface plot of the interpolated electric field magnitude as a function of $\theta$ and frequency

$$F(\theta,\ \phi,\ s) = \frac{N_0(\theta,\ \phi) + N_1(\theta,\ \phi)s + N_2(\theta,\ \phi)s^2 + \cdots + N_n(\theta,\ \phi)s^n}{D_0(\theta,\ \phi) + D_1(\theta,\ \phi)s + D_2(\theta,\ \phi)s^2 + \cdots + D_{d-1}(\theta,\ \phi)s^{d-1} + s^d} \tag{11}$$

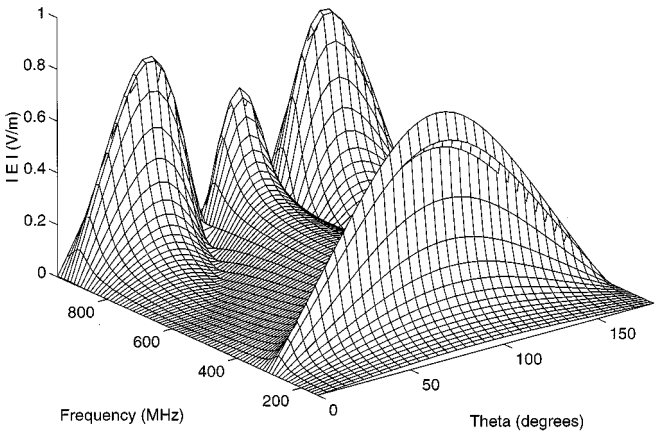


Fig. 1. Electric field magnitude as a function of spatial variable $\theta$ and frequency for a 0.5-m dipole obtained using hybrid MBPE technique.

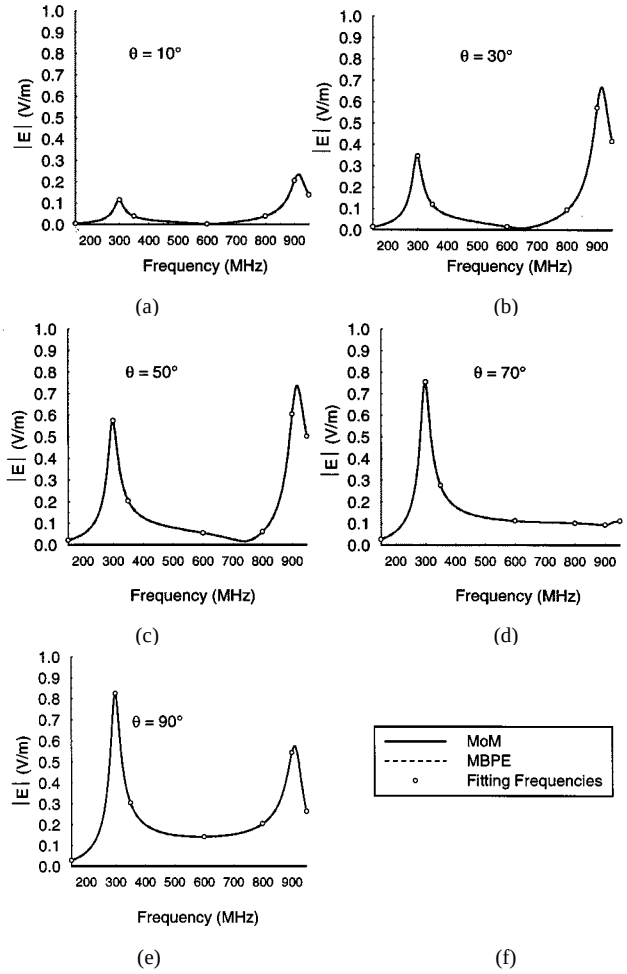


Fig. 2. Comparison of the electric field frequency response of a 0.5-m dipole using MoM and MBPE at $\theta = 10$, 30, 50, 70, and 90° with the seven fitting frequencies, 150, 300, 350, 600, 800, 900, and 950 MHz, shown as circles.

is shown in Fig. 1. Fig. 2 shows a series of plots of the electric field magnitude versus frequency for this dipole at $\theta = 10$, 30, 50, 70, and 90°, with comparisons being made between the MoM frequency spectra and the spectra obtained via MBPE.

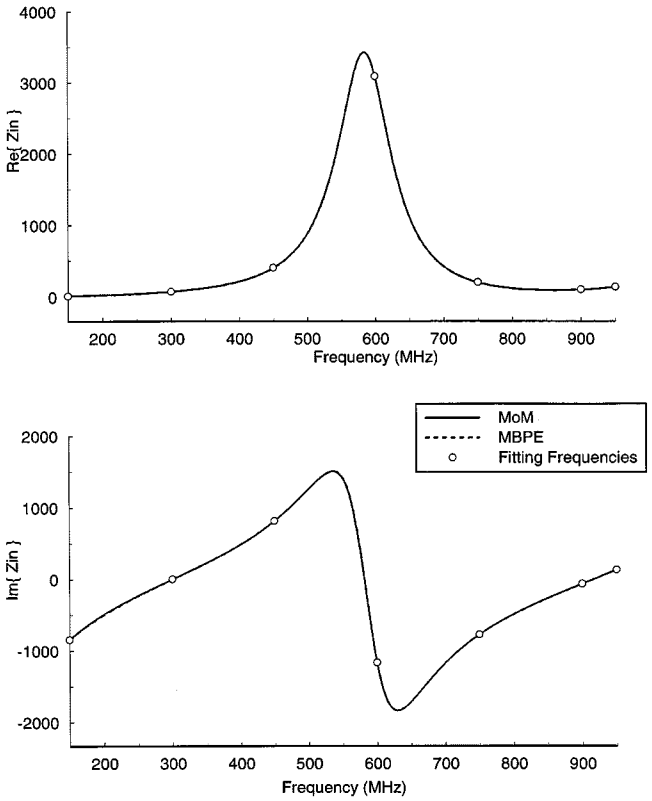


Fig. 3. A comparison of $\mathrm{Re}\{Z_{\mathrm{in}}\}$ and $\mathrm{Im}\{Z_{\mathrm{in}}\}$ for a 0.5-m dipole computed using MoM and MBPE, with the seven fitting frequencies, 150, 300, 450, 600, 750, 900, and 950 MHz, shown as circles.

As can be seen from Fig. 2, the two curves are nearly graphically indistinguishable. In this case, only seven fitting frequencies were required for the MBPE technique. The actual fitting frequencies that were used are indicated by circles on the plots contained in Fig. 2. The plots in this figure also show that one of the fitting frequencies chosen coincides with the half-wave resonance of the 0.5-m dipole at 300 MHz. Although it has been demonstrated by Miller [4] that spectral domain MBPE does not necessarily require that resonances be sampled in order for their structure to be preserved, in this case choosing 300 MHz as a sampling frequency seemed a natural and beneficial choice to make. The application intended here is the interpolation of a known set of data rather than the estimation of an entire set of data from a sparse set of measurements, so minimizing the number of sampling frequencies is highly desirable. Placing fitting frequencies at or very near to resonances insures that the interpolation accurately preserves the structures and locations of these important features while still allowing a minimum number of spectral-domain sampling points to be used.

MoM-generated and MBPE-interpolated curves of the real and imaginary parts of the input impedance versus frequency for the 0.5-m dipole example are shown in Fig. 3. The seven fitting frequencies are shown as circles. The fits to these impedance curves obtained using MBPE, as shown in Fig. 3, are nearly identical to the impedance values calculated by MoM. Using this interpolated impedance and the MBPE interpolated electric field values, the gain pattern for the antenna as a function of $\theta$

and frequency was determined (see Fig. 4). A series of six pattern cuts at the frequencies 300, 500, 600, 720, 800, and 933 MHz are shown in Fig. 5, which further demonstrate the excellent agreement between the MBPE and MoM results. Three of these frequencies, 500, 720, and 933 MHz, are not among the fitting frequencies that were selected.

We note here that in the case of the simple 0.5-m dipole, it was only necessary to assume a spatial dependence for the numerator coefficients of the fitting model given in (6). This property may be attributed to the fact that the location of the poles for antenna radiation patterns should be dictated solely by the geometry of the antenna structure [14], [15]. This also suggests that the required number of sampling points for this problem may be reduced by an amount equal to $kd$ (in this case $kd = 14$). Hence, by taking advantage of this property, the required number of coefficients for the fitting model may be reduced from 56 to 42.

The second example used to demonstrate this new MBPE procedure was a three-element Yagi array antenna, designed for optimized operation at 485 MHz. The driver length was chosen to be 0.453 $\lambda$, the reflector length 0.479 $\lambda$, the director length 0.451 $\lambda$, the element spacing was selected as 0.25 $\lambda$, and the wire radius was chosen to be 0.00016 $\lambda$. The Yagi is located in the $y$–$z$ plane with the elements parallel to the $y$-axis. An MBPE fitting model of the form (11) was chosen in this case because the radiation patterns for the Yagi will have a spatial dependence on both $\theta$ and $\phi$ as well as a frequency dependence. The angular variation of the rational function numerator and denominator coefficients were modeled using binomial expansions of the type proposed in (12) and (13), respectively. Unlike the dipole, the radiated field in this case has both $E_\theta$ and $E_\phi$ components. Each component was interpolated separately and then combined using (17)–(20) in order to produce the corresponding gain patterns. In this case, it was found necessary to assume an angular dependence for both the numerator and denominator coefficients.

The $E_\theta$ interpolation used a Padé rational function with numerator order $n = 2$ and denominator order $d = 2$, and the spatial dependence in both $\theta$ and $\phi$ for each of the five unknown complex coefficients was modeled using binomial functions with $P_n = 8$. The frequency domain sampling was done at only five frequencies (i.e., 470, 475, 485, 495, and 500 MHz), which were chosen to equal the number of unknown Padé rational function coefficients. The class eight binomial has 45 unknown coefficients and there is one binomial function for each Padé coefficient, resulting in an overall total of $45 \times 5 = 225$ unknown coefficients to be determined for the $E_\theta$ interpolation. A grid of 196 spatial sampling points was created by choosing the values $\theta = \phi = 0$, 10, 20, 40, 60, 70, 90, 100, 120, 140, 160, 170, 175, and 180° (i.e., $N\theta = N\phi = 14$). It was found that sufficient accuracy could be achieved by using as few as five sampling frequencies. Hence, a total of $196 \times 5 = 980$ sampling points was required to estimate the coefficients of the fitting model. In this case, a least-squares approach was implemented in order to solve the resulting matrix equation for the desired coefficients. Comparisons were made at several frequencies, which showed excellent agreement between the MoM-calculated and MBPE-interpolated electric fields. For the $E_\phi$ interpolation, the same numerator and denominator orders for the Padé rational function were used, but this time a class $P_n = 7$ binomial function was sufficient to model the

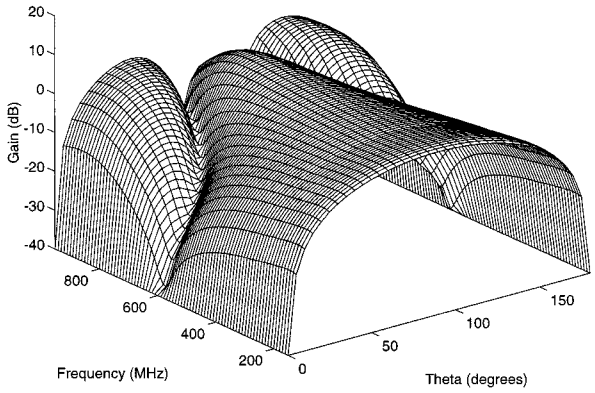


Fig. 4. Gain as a function of spatial angle $\theta$ and frequency for a 0.5-m dipole computed using MBPE.

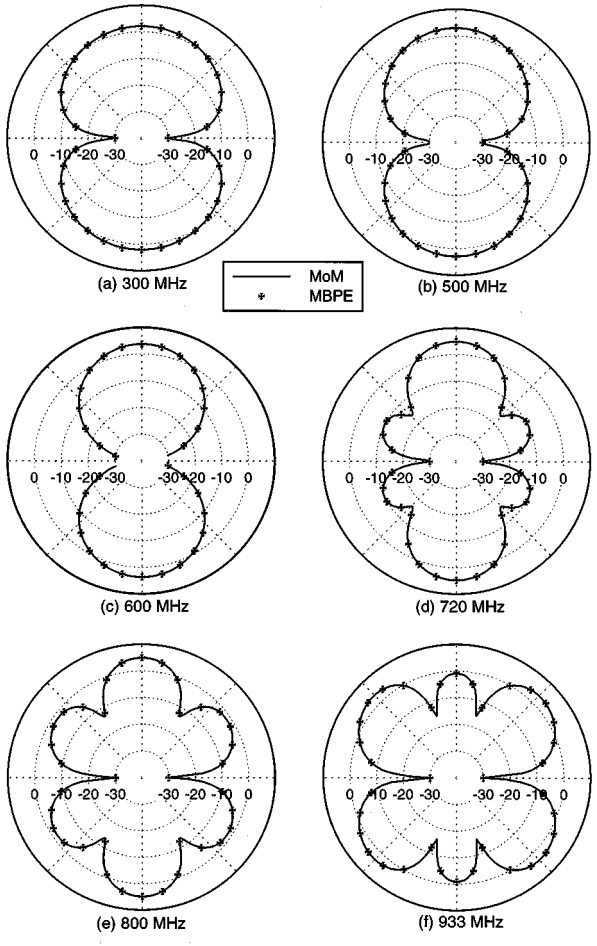


Fig. 5. Principle plane cuts of the gain pattern for a 0.5-m dipole at (a) 300 MHz; (b) 500 MHz; (c) 600 MHz; (d) 720 MHz; (e) 800 MHz; and (f) 933 MHz, with the MoM pattern indicated by the solid curve and the MBPE determined gain represented by crosses.

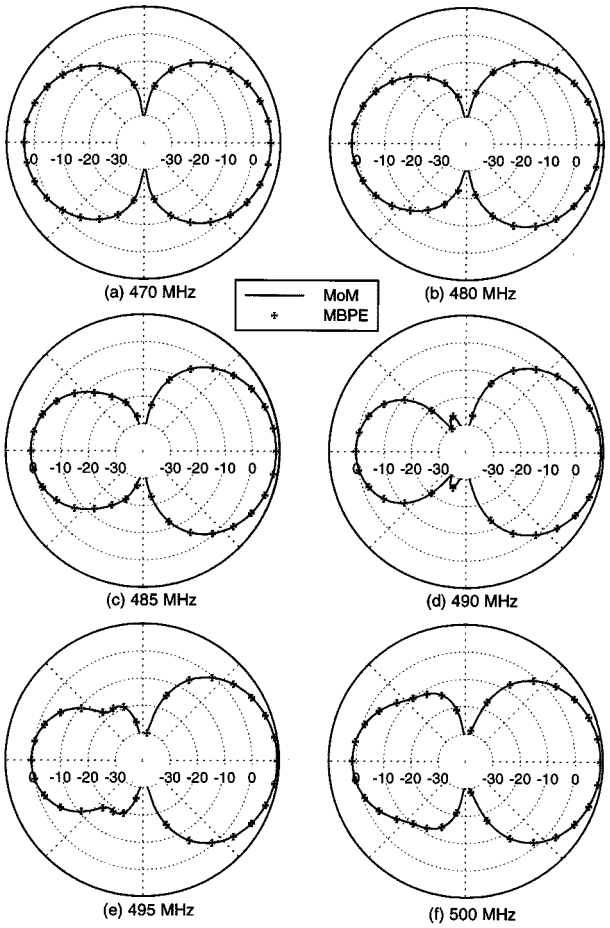


Fig. 6. $E$-plane cuts of the gain pattern for a three-element Yagi array at (a) 470 MHz; (b) 480 MHz; (c) 485 MHz; (d) 490 MHz; (e) 495 MHz; and (f) 500 MHz, with the MoM pattern indicated by the solid curve and the MBPE determined gain represented by crosses.

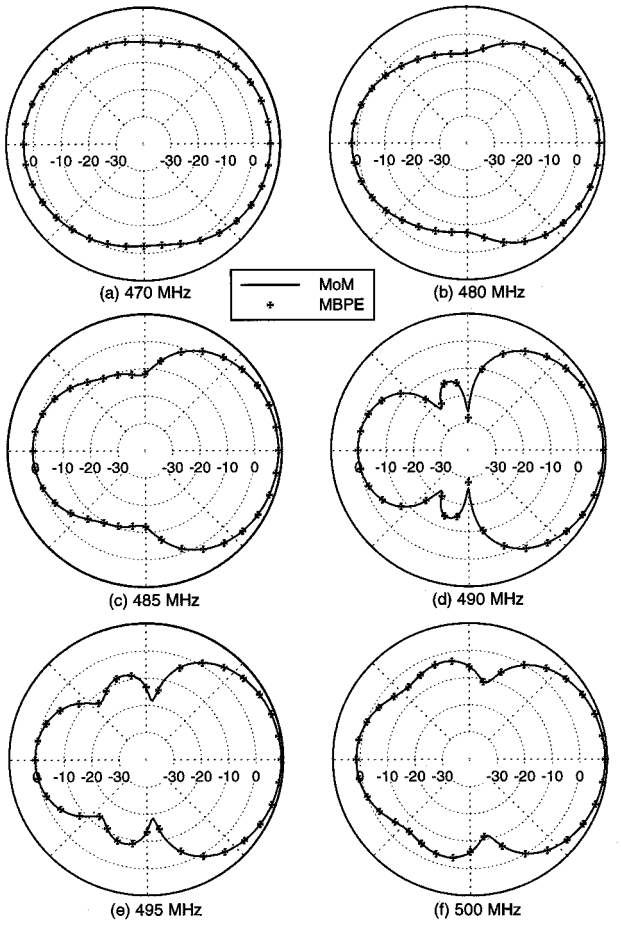


Fig. 7. $H$-plane cuts of the gain pattern for a three-element Yagi array at (a) 470 MHz; (b) 480 MHz; (c) 485 MHz; (d) 490 MHz; (e) 495 MHz; and (f) 500 MHz, with the MoM pattern indicated by the solid curve and the MBPE determined gain represented by crosses.

spatial variation, resulting in a total of $36 \times 5 = 180$ unknown coefficients. The sampling scheme is the same as that used for the $E_\theta$ component and, as before, the interpolation produced results in good agreement with electric field values calculated using the more rigorous MoM approach. It should be noted that contrary to the statement made for the 0.5-m dipole example that the denominator coefficients of the Padé rational function do not require spatial dependence, in this case it was necessary to include dependence on both $\theta$ and $\phi$ in the denominator in order to obtain accurate results. This is due to the fact that very little of the resonant structure for this Yagi antenna is present in the 470–500 MHz frequency range under consideration, so the spatial variable dependence in the denominator is necessary to compensate for this missing information.

After the required interpolations for both the $E_\theta$ and $E_\phi$ components of the radiated electric field as well as the input impedance $Z_{\text{in}}$ were performed, the corresponding gain pattern of the Yagi could then be determined using (17). Figs. 6 and 7 show $E$-plane and $H$-plane pattern cuts of the resulting gain patterns for the Yagi at six different frequencies, 470, 480, 485, 490, 495, and 500 MHz. These plots clearly demonstrate the ability of the MBPE interpolation technique to accurately reproduce the evolving structure of the antenna gain patterns, including the changing front-to-back ratio and the appearance of sidelobes above the design frequency.

The two examples considered above serve to illustrate how this new MBPE technique may be used to achieve a significant reduction in the amount of generated and stored data required to accurately reproduce antenna radiation patterns, especially those which vary with frequency. For instance, the MBPE approach only required storing 42 complex coefficients in order to generate the plot shown in Fig. 1 for the 0.5-m dipole. On the other hand, the conventional approach for generating this plot would require radiation pattern data to be calculated via a MoM code in 10-MHz increments from 150 to 950 MHz and, at each frequency, over a range of $\theta$ from 0 to 180°, with at least 2° angular resolution. This would make it necessary to store a total of 7371 complex data points as opposed to only 42 in the MBPE case. Furthermore, the MBPE technique has the added advantage of being able to reproduce radiation patterns at any desired frequency within the fitting-model range and with any desired an-

gular resolution. These properties make the MBPE method particularly attractive for use in the creation of large antenna radiation pattern databases, where all the necessary information can be stored in compressed form.

A second important feature of this new hybrid MBPE technique is that when used in conjunction with MoM codes, it could potentially reduce the required computation time for antenna radiation patterns by several orders of magnitude depending upon the size of the MoM problem space. Complex MoM antenna models consisting of several thousand wire segments often require many hours to calculate radiation patterns for a single frequency. If it is desired to calculate these patterns over a large range of frequencies, then the required calculation time could rapidly become prohibitive. By using the MBPE technique described in this paper, however, which uses reduced order fitting models, only the data needed for the interpolation would have to be generated. Radiation patterns could then be efficiently interpolated at any other desired frequency within the range of the fitting model. An adaptive sampling scheme has been introduced by Miller [7], [8], [16], which uses overlapping fitting models to find the most suitable positioning of sampling points for a given Padé approximation. Adaptive sampling would be very useful for the procedure described above, since it would predict which frequency data points would have to be generated in advance, thus removing any reliance on a trial-and-error sampling technique. Similarly, for the spatial domain expansion functions, an appropriate order can be found by determining what order function most accurately fits the radiation pattern at the highest desired frequency. This is true because the radiation pattern for an antenna is generally more complicated at higher frequencies than it is at lower frequencies. Bose has shown in [17] and [18] that a recursion relationship exists for the denominator of the Padé rational function that makes it possible to efficiently increase the order of the frequency domain interpolation without having to reevaluate the often large Padé matrix equation. These techniques, when taken together, would make the use of the MBPE approach described in this paper applicable for the efficient calculation of antenna radiation patterns for problems which ordinarily would have very large computational domains. This aspect of the hybrid MBPE technique is currently being investigated by the authors.

## IV. Conclusions

An approach has been introduced in this paper whereby the Padé rational function fitting model commonly used for MBPE in the frequency domain can be easily modified to include spatial dependence in its numerator and denominator coefficients. It was demonstrated that generalized MBPE techniques of this type provide extremely powerful tools for interpolating antenna radiation patterns in both the frequency and spatial domains simultaneously. This new interpolation technique was applied to two examples, a 0.5-m dipole antenna and a three-element Yagi array and, in each case, the modified Padé rational function yielded excellent agreement with the exact results calculated using MoM. The MBPE method outlined in this paper offers two important advantages—one being large compression ratios for data storage of antenna radiation patterns and the other a significant decrease in the amount of time required to process antenna models with large computational domains.

## Acknowledgment

The authors would like to thank E. Miller, R. Mittra, P. Werner, J. Zmyslo, and N. Bose for their assistance.

## References

[1] P. Lancaster and K. Salkauskas, *Curve and Surface Fitting: An Introduction*. New York: Academic, 1986, p. 280.

[2] E. K. Miller, "Model-based parameter estimation in electromagnetics—I: Background and theoretical development," *Applied Computational Electromagnetics Society Newsletter*, vol. 10, no. 3, pp. 40–63, 1995.

[3] ——, "Model-based parameter estimations in electromagnetics—Part I: Background and theoretical development," *IEEE Antennas Propagat. Mag.*, vol. 40, pp. 42–52, 1998.

[4] ——, "Model-based parameter estimation in electromagnetics—Part II: Applications to EM observables," *Appl. Computat. Electromagn. Soc. Newsletter*, vol. 11, no. 1, pp. 35–56, 1996.

[5] ——, "Model-based parameter estimation in electromagnetics—Part III: Applications to EM integral equations," *Appl. Computat. Electromagn. Soc. J.*, vol. 10, no. 3, pp. 9–29, 1995.

[6] ——, "Using model-based parameter estimation to estimate the accuracy of numerical models," in *12th Annu. Rev. Progress Appl. Computat. Electromagn.*. Monterey, CA, 1996, pp. 588–595.

[7] ——, "Minimizing the number of frequency samples needed to represent a transfer function using adaptive sampling," in *12th Annu. Rev. Progress Appl. Computat. Electromagn.*. Monterey, CA, pp. 1132–1139.

[8] ——, "Using windowed, adaptive sampling to minimize the number of field values needed to estimate radiation and scattering patterns," in *14th Annu. Rev. Progress Appl. Computat. Electromagn.*, vol. 2, 1998, pp. 958–963.

[9] R. Roberts and D. A. McNamara, "Interpolating radiation patterns using Prony's method," in *Proc. Symp. Antennas Propagat. Microwave Theory Tech.*. Stellenbosch, South Africa, 1994, pp. 151–154.

[10] W. H. Press, B. P. Flannery, S. A. Teukolsky, and W. T. Vetterling, *Numerical Recipes: The Art of Scientific Computing*. New York: Cambridge Univ. Press, 1986, p. 818.

[11] R. J. Allard, D. H. Werner, J. S. Zmyslo, and P. L. Werner, "Spectral domain interpolation of antenna radiation patterns using model-based parameter estimation and genetic algorithms," in *14th Annu. Rev. Progress Appl. Computat. Electromagn.*. Monterey, CA, 1998, pp. 964–971.

[12] ——, "Model-based parameter estimation of antenna radiation pattern frequency spectra," in *Proc. IEEE Antennas Propagat. Soc. Int. Symp.*, vol. 1, Atlanta, GA, June 1998, pp. 62–65.

[13] W. L. Stutzman and G. A. Thiele, *Antenna Theory and Design*. New York: Wiley, 1981, p. 598.

[14] C. E. Baum, "Emerging technology for transient and broad-band analysis and synthesis of antennas and scatterers," *Proc. IEEE*, vol. 64, pp. 1598–1615, Nov. 1976.

[15] J. N. Brittingham, E. K. Miller, and J. L. Willows, "Pole extraction from real-frequency information," *Proc. IEEE*, vol. 68, pp. 263–273, Feb. 1980.

[16] E. K. Miller, "Computing radiation and scattering patterns using model-based parameter estimation," in *Proc. IEEE Antennas Propagat. Soc. Int. Symp.*, vol. 1, Atlanta, GA, June 1998, pp. 66–69.

[17] N. K. Bose, *Digital Filters: Theory and Applications*. Malabar, FL: Krieger, 1985, p. 508.

[18] N. K. Bose and S. Basu, "Theory and recursive computation of 1-D matrix Padé approximants," *IEEE Trans. Circuits Syst.*, vol. 27, pp. 323–325, Apr. 1980.

**Douglas H. Werner** (S'81–M'89–SM'94) received the B.S., M.S., and Ph.D. degrees in electrical engineering from The Pennsylvania State University, State College, PA, in 1983, 1985, and 1989, respectively, and the M.A. degree in mathematics at the same university in 1986.

He is an Associate Professor at the Department of Electrical Engineering, The Pennsylvania State University. He is a member of the Communications and Space Sciences Laboratory (CSSL) and is affiliated with the Electromagnetic Communication Research Laboratory, The Pennsylvania State University. He is also a Senior Research Associate in the Communications Science and Technology Division of the Applied Research Laboratory, The Pennsylvania State University. He is an associate editor of *Radio Science*. He has published numerous technical papers and proceedings articles and is the author of six book chapters. He is the coeditor of *Frontiers in Electromagnetics* (Piscataway, NJ: IEEE Press, 2000). His research interests include theoretical and computational electromagnetics with applications to antenna theory and design, microwaves, wireless and personal communication systems, electromagnetic wave interactions with complex materials, fractal and knot electrodynamics, and genetic algorithms.

Dr. Werner is a member of the American Geophysical Union (AGU), URSI Commissions B and G, the Applied Computational Electromagnetics Society (ACES), Eta Kappa Nu, Tau Beta Pi, and Sigma Xi. He was presented with the 1993 Applied Computational Electromagnetics Society (ACES) Best Paper Award and was also the recipient of a 1993 International Union of Radio Science (URSI) Young Scientist Award. In 1994 he received the The Pennsylvania State University Applied Research Laboratory Outstanding Publication Award. He has also received several letters of commendation from the Department of Electrical Engineering, The Pennsylvania State University, for outstanding teaching and research.

**Rene J. Allard** was born in Hartford, CT, on April 6, 1974. He received the B.A. degree in physics and astronomy from Boston University, Boston, MA, in 1996, and the M.S. degree in electrical engineering from The Pennsylvania State University, State College, PA, in 1998. He is currently working toward the Ph.D. degree in electrical engineering at the same university.

He is currently a Research Assistant in the Communications Science and Technology Division of the Applied Research Laboratory at The Pennsylvania State University. His research interests are in the field of computational electromagnetics, including the analysis and design of conformal antennas and electromagnetic optimization techniques such as model-based parameter estimation and genetic algorithms.